

# Biodendrimer-Based Hydrogel Scaffolds for Cartilage Tissue Repair

Serge H. M. Söntjens,<sup>†</sup> Dana L. Nettles,<sup>‡</sup> Michael A. Carnahan,<sup>§</sup> Lori A. Setton,<sup>‡</sup> and Mark W. Grinstaff<sup>\*†</sup>

*Departments of Chemistry and Biomedical Engineering, Boston University, Metcalf Center for Science and Engineering, 590 Commonwealth Avenue, Boston, Massachusetts 02215, Department of Biomedical Engineering, Duke University, Durham, North Carolina, and Department of Ophthalmology, Duke University Medical Center, Durham, North Carolina*

*Received September 9, 2005; Revised Manuscript Received October 9, 2005*

Photo-crosslinkable dendritic macromolecules are attractive materials for the preparation of cartilage tissue engineering scaffolds that may be optimized for in situ formation of hydrated, mechanically stable, and well-integrated hydrogel scaffolds supporting chondrocytes and chondrogenesis. We designed and synthesized a novel hydrogel scaffold for cartilage repair, based on a multivalent and water-soluble tri-block copolymer consisting of a poly(ethylene glycol) core and methacrylated poly(glycerol succinic acid) dendrimer terminal blocks. The terminal methacrylates allow mild and biocompatible photo-crosslinking with a visible light, facilitating in vivo filling of irregularly shaped defects with the dendrimer-based scaffold. The multivalent dendrimer constituents allow high crosslink densities that inhibit swelling after crosslinking while simultaneously introducing biodegradation sites. The mechanical properties and water content of the hydrogel can easily be tuned by changing the biodendrimer concentration. In vitro chondrocyte encapsulation studies demonstrate significant synthesis of neocartilaginous material, containing proteoglycans and type II collagen.

## Introduction

Cartilage degeneration due to osteoarthritis or trauma is a common condition, afflicting millions of individuals. The restoration of damaged cartilaginous tissue is consequently of considerable clinical interest. The degeneration of articular cartilage, meniscus, and intervertebral disk may lead to severe and debilitating pain in patients. Due to the low regenerative capacity of native cartilage, injuries to these tissues are generally retained for many years and may eventually lead to more severe secondary damage.<sup>1,2</sup> At present, the available clinical treatments include the chronic use of antiinflammatory drugs, transplantation, total joint replacement, discectomy, joint fusion, or chondrocyte transplantation.<sup>2</sup> These clinical options are often inadequate long-term, and thus, alternative treatment based on tissue engineering strategies may significantly improve patient care. Consequently, strategies based on exogenous scaffolds, both natural and synthetic, have been investigated for cartilage repair. Natural polymers evaluated for cartilage repair, with or without cellular supplementation, include alginate, fibrin, chitosan, hyaluronan, and type I and type II collagen gels.<sup>3–11</sup> In addition, synthetic biocompatible materials such as poly(glycolic acid), poly(lactide), poly(caprolactone), and various other polyester copolymers have been studied widely as scaffolds.<sup>12–15</sup> Hydrogel systems based on crosslinked poly(ethylene glycol) derivatives have also received considerable attention.<sup>16–19</sup>

Hydrogel materials are particularly successful as tissue engineering scaffolds because they are water-saturated turgid networks that mimic the three-dimensional environment of cells

in native cartilaginous tissues. In addition, the high water content allows for adequate diffusion of nutrients and oxygen to and waste products and carbon dioxide from the cells which may have a positive influence on the metabolic activity of cells within the scaffold material.

The requirements for a successful tissue-engineering scaffold for cartilage repair are complex and extend beyond basic biocompatibility and low toxicity. As a stress-absorbing tissue, the mechanical properties of cartilage define its function in the body and are thus an important design criterion for a cartilage repair material. Cartilaginous tissues, including articular cartilage, meniscus, and intervertebral disk, are porous, water saturated viscoelastic materials that exhibit high mechanical stiffness; however, the mechanical properties reflected in the compressive and (dynamic) shear moduli strongly depend on the specific tissue-type (Table 1).

Restoring mechanical function at the time of cartilage repair is highly desirable for maintaining tissue and joint function, reducing inflammation at the trauma site, and maintaining the environment governing cell metabolism and matrix homeostasis.<sup>20</sup> Consequently, there is significant interest in manipulating the mechanical properties of a biomaterial during synthesis and implantation, to obtain a functional scaffold that will support load and permit integration with native tissue. In addition to mechanical function, several other properties may affect scaffold success, including diffusion of large and small molecules, porosity, surface properties, tissue adhesion, morphology, and (bio)degradation kinetics.

Photo-crosslinkable hydrogels based on poly(ethylene glycol) dimethacrylate have shown considerable promise as tissue-engineering scaffolds.<sup>17–19</sup> The in situ photo-crosslinking ability of these systems is highly desirable in a cartilage tissue-engineering application for a variety of reasons. First, it allows the uncrosslinked macromer solution to be mixed with cells

\* To whom correspondence should be addressed. Tel: (617) 358-3429. Fax: (617) 343-6466. E-mail: mgrin@bu.edu.

<sup>†</sup> Boston University.

<sup>‡</sup> Duke University.

<sup>§</sup> Duke University Medical Center.

**Table 1.** Mechanical Properties of a Selection of Native Cartilaginous Tissues in Humans<sup>47–50</sup>

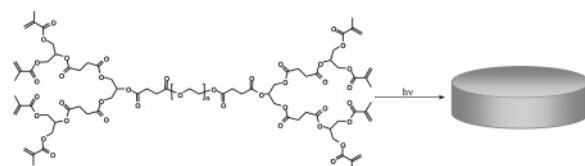
	compressive modulus $E/\text{kPa}$	complex shear modulus $ G^* /\text{kPa}$	phase angle $\delta/^\circ$
articular cartilage	600	440, 600–1000	13
meniscus	n/a	100	22
annulus fibrosus	111, 76	540	n/a
nucleus pulposus	5.8	7–21	23–31

or soluble factors, such as growth factors or cytokines, prior to delivery to the defect site. Second, the uncrosslinked macromer solution can easily flow into irregularly shaped defects common to damaged or diseased cartilage, facilitating integration with the surrounding native tissue. Third, the liquid state of the macromer solution allows access to surgically inaccessible trauma sites via endoscope-assisted (micro)surgery. Last, these materials, once crosslinked in situ, provide immediate adhesion and mechanical integrity to the defect site at the time of implantation.

A limitation of the poly(ethylene glycol) dimethacrylate hydrogels, however, is the lack of (bio)degradation, which hampers long-term viability of incorporated cells and inhibits formation of neocartilage throughout the scaffold. The introduction of degradation sites into these hydrogels, allowing chondrocytes to degrade the scaffold while extracellular matrix is deposited, is one solution to this problem. It was shown recently by Hubbell and Anseth that both linear oligopeptides<sup>21</sup> and linear esters<sup>22–24</sup> allow biodegradation when incorporated into the scaffold design. It is, however, crucial that degradation of the matrix material is tuned to the synthesis of extracellular matrix in such a way that the mechanical properties of the site are not compromised.<sup>25</sup>

Hydrogels derived from dendrimer-based polymers offer an alternative to those based on a linear structure. Dendrimers are highly branched, well-defined macromolecules that are ideal compounds for the assembly of such materials.<sup>26–39</sup> Dendritic polymers provide a multivalent and modular base for the design and optimization of novel macromers for tissue engineering scaffold applications. The branched structure allows considerable degradation before the crosslinked network breaks down, maintaining mechanical integrity during degradation. The multivalency of branched structures also allows higher crosslink densities at low concentrations compared to linear functionalized polymers, providing the potential to achieve the seemingly conflicting requirements of high mechanical strength and high water content required for cartilage repair. In addition, the well-defined nature of these macromolecules allows analysis of structure–property relationships between the molecular features of the macromers and the mechanical and physiochemical properties of the hydrogel constructs, allowing subsequent structure-based optimization of these constructs for specific applications.

We previously have reported biocompatible dendrimers, or biodendrimers, constructed from moieties known to be biocompatible.<sup>40</sup> Tissue adhesives based on methacrylated block copolymers, consisting of a PEG core and biodendrimer wedges synthesized from glycerol and succinic acid, display excellent corneal tissue adhesion and show considerable promise as an ocular sealant for sutureless eye-surgery.<sup>41</sup> An investigation of these materials as in situ photo-crosslinkable scaffold materials for articular cartilage tissue engineering is presented herein (Figure 1). Results are reported for the physical characterization of the biodendrimer scaffolds including swelling, mechanical,

**Figure 1.** Photo-crosslinkable PEG<sub>3400</sub>-(PGLSA-MA<sub>4</sub>)<sub>2</sub> macromer **1** for hydrogel formation.

and degradation properties, as well as the ability of the hydrogel to support articular chondrocytes and extracellular matrix synthesis in vitro.

## Experimental Section

**General.** All chemicals and culture media were used as received and were stored at room temperature, in the dark, or 4 °C where appropriate. All errors are reported as mean values  $\pm$  one standard deviation. The differences between samples were evaluated with one-way ANOVA with a Tukey HSD post-hoc test. All macromer concentrations were reported as percentage weight macromer per weight solvent; macromer solutions showed densities of  $1.04 \pm 0.02$ ,  $1.03 \pm 0.01$ , and  $1.04 \pm 0.03$  g/mL for solutions at 7.5, 10, and 15% macromer **1** in phosphate buffered saline (PBS), respectively. Chondrocyte growth medium consisted of Dulbecco's modified Eagle's medium (DMEM) supplemented with 10% fetal bovine serum (FBS), 2.5 mg/mL phosphate-C, and 5 mL penicillin/streptomycin (Invitrogen, Carlsbad CA). Washing medium consisted of DMEM high glucose with L-glutamine, 110 mg/mL sodium pyruvate with pyridoxine HCl, 3.3 mL/L 300 $\times$  stock gentamycin, 10 mL/L 100 $\times$  stock kanamycin, and 5 mL/L 200 $\times$  fungizone (Invitrogen, Carlsbad CA).

**Hydrogel Synthesis.** The PEG<sub>3400</sub>-(PGLSA-MA<sub>4</sub>)<sub>2</sub> macromer **1** was synthesized from poly(ethylene glycol) with a weight average molecular weight of 3400 g/mol as a core and biodendrimers based on glycerol (GL) and succinic acid (SA), as described previously by Carnahan et al.<sup>42</sup> To evaluate the mechanical properties of the crosslinked biodendrimer macromer **1** solutions at 7.5, 10, 15, and 20% w/w in DPBS (Dulbecco's Phosphate Buffered Saline, Invitrogen), the solutions were first mixed with 5  $\mu$ L of the photoinitiator solution (0.1% eosin-Y, 4% *N*-vinyl-2-pyrrolidinone, and 40% triethanolamine in PBS, Invitrogen). The resulting solution was subsequently crosslinked in cylindrical molds (dia 8 mm,  $h = 2$  mm) with long-wave UV (30 min), a filtered Xenon arc lamp (2 min with a Spectra-Physics/Oriel, 300W Xe lamp with filter #59070, yielding  $\sim 100$  mW at 510 nm), or an argon laser (60 s at 514 nm, 200 mW, Ultima SE 120V, Lumenis), to form a three-dimensional turgid hydrogel. The resulting pellets were stored in PBS at room temperature or 37 °C. Due to the absence of significant swelling, all concentrations reported here are initial macromer concentrations, uncorrected for swelling after crosslinking.

**Mechanical Testing.** Cylindrical hydrogel samples for dynamic mechanical testing were prepared by crosslinking biodendrimer solutions at 7.5, 10, 15, and 20% w/w with the eosin-based initiator mentioned above in cylindrical molds (dia = 8 mm,  $h = 2$  mm) with long-wave UV (30 min) or an argon-ion laser (514 nm, 200 mW, 60 s, Ultima SE 120V, Lumenis, Santa Clara, CA). The mechanical properties were similar for both photo-crosslinking methods. The samples were removed from the molds and were subsequently allowed to equilibrate in PBS solution for 3 days at room temperature. After equilibration, the samples were investigated on a strain-controlled rheometer (ARES, Rheometrics Scientific) with torque (0.2–200 gf  $\text{cm}^{-1}$ ) and normal force (0–2000 gf) transducers with a parallel-plate geometry with stainless steel porous platens (50% porosity, 40–60  $\mu$ m pore size) immersed in a PBS bath. Data for torque, normal force, and torsional displacement were recorded by data acquisition software (Rhios Orchestrator 6000, Rheometric Scientific). The undeformed diameter  $d$  of the samples was determined with a micro caliper. The samples were subsequently centered on the lower platen, and the top

platen was lowered to contact the sample until a small contact force was applied ( $\sim 0.02$  N). The reference undeformed thickness of the sample ( $h_0$ ) was determined from the axial displacement data at that position. A dynamic frequency sweep was performed from 0.1 to 100 Hz at a maximum strain amplitude of 0.05. Based on the assumption of linear viscoelastic behavior, the complex modulus ( $|G^*|$ ) and the storage ( $G'$ ) and loss ( $G''$ ) moduli were determined from the data. The loss angle  $\delta$  was calculated from  $\delta = \tan^{-1}(G''/G')$ , and provides a relative measure of the viscous versus elastic effects in the material. No significant frequency dependence was detected in the observed frequency range. The frequency independent dynamic shear modulus ( $|G^*|$ ), storage modulus ( $G'$ ), loss modulus ( $G''$ ), and the loss angle ( $\delta$ ) are consequently shown as average values from data at 5–10 rad/s, allowing estimation of the errors inherent in the experiment from the scatter of the data. A series of compressive stress-relaxation experiments were performed on similar samples in strain increments of 5% up to 20% maximum compressive strain [ $\epsilon = (h - h_0)/h_0$ ], to determine the equilibrium compressive modulus. After each increment, the compressive stress (normal force/sample area) was recorded for up to 30 min or until the deviation of the data was less than 1% for 30 s. The compressive moduli were subsequently determined by linear regression of the equilibrium stress versus strain data; errors were estimated from the standard deviation. The hydrogel samples, especially at lower macromer concentration, were rather fragile, and not all samples survived transportation and mounting. As a result, the dynamic frequency sweep experiments were recorded with different sample sizes for different macromer concentrations (7.5%:  $n = 2$ , 10%:  $n = 3$ , 15%:  $n = 6$ , and 20%:  $n = 6$ ). The compressive strain experiments were all performed with  $n = 2$ .

**Chondrocyte Encapsulation.** Chondrocytes were isolated from the femoral condyles of skeletally immature porcine knees (3–5 months) using an enzymatic digestion protocol described previously.<sup>43</sup> Cells were washed with washing medium and were subsequently re-suspended at  $2 \times 10^7$  cells/mL in either a 7.5% w/w or 15% w/w biodegradable solution with 5% of the photoinitiator system. Samples (100  $\mu$ L) of the cell suspensions were placed in cylindrical molds (dia = 8 mm,  $h = 2$  mm) and cross-linked with an argon-ion laser (514 nm, 200 mW, 60 s, Ultima SE 120V, Lumenis, Santa Clara, CA) to create cell-gel constructs. No loss in cell viability is observed under these photocrosslinking conditions. These constructs were placed in individual wells and cultured in chondrocyte culture medium in a humidified atmosphere at 37 °C with 5% CO<sub>2</sub>. The culture medium was replaced every 3 days. Unseeded constructs incubated under the same conditions served as controls. Constructs containing cells were harvested at 2, 4, and 12 weeks ( $n = 3$ ) and processed for histology. Control constructs without chondrocytes were harvested at 12 weeks ( $n = 2$ ) and studied similarly.

**Histology and Immunohistochemistry.** Cell-gel constructs were placed in paraformaldehyde for 30 min, followed by dehydration in a graded series of ethanol prior to embedding in paraffin. Paraffin-embedded sections were stained with H&E, Safranin-O, or Masson's Trichrome for histological evaluation. Sections were also immunolabeled for the presence of types I (Sigma C2456) and II (DSHB II-II6B3) collagen, with visualization via a horseradish-conjugated secondary antibody.

Images were taken from stained sections, randomized, and graded by three readers for cell arrangement, proteoglycan, and collagen staining (blind study), as well as collagen-specific staining from immunolabeled sections. A total of 9 features were graded (0–2) for a total possible score of 18. Scores were totaled for each macromer concentration at 2 and 4 weeks and averaged across readers (see the Supporting Information for grading scale).

**Hydrogel Swelling and Degradation.** Cylindrical hydrogel samples for swelling and degradation testing were prepared by cross-linking biodegradable solutions at 7.5, 10, and 15% w/w ( $n = 3$ ) mixed with the photoinitiating system in cylindrical molds (dia = 8 mm,  $h = 2$  mm) with a filtered Xenon arc lamp (2 min with a Spectra-Physics/Oriel 300W Xe lamp with filter #59070, yielding  $\sim 100$  mW at 510

nm). The crosslinked hydrogel pellets were subsequently stored at 37 °C in phosphate buffered saline (PBS, Invitrogen) or chondrocyte cell culture medium, both supplemented with 0.1% NaN<sub>3</sub> to prevent bacterial or fungal infection. The weight of the samples was measured over a period of 35 days, and was normalized by the weight of the samples immediately after crosslinking. The weight change over time was used as an estimate of swelling and hydrogel degradation in cell culture medium or PBS, in the absence of chondrocytes.

## Results

**Hydrogel Synthesis.** Concentrations of macromer **1** from 5 to 20% w/w were observed to crosslink uniformly within the molds. The hydrogel samples formed from biodegradable solutions below 7.5% w/w were very fragile after crosslinking, however, and were consequently difficult to investigate. Thus, we limited our study to macromer concentrations from 7.5 to 20%. The appearance of the crosslinked hydrogel pellets was dependent on macromer concentration. Equilibrated hydrogel constructs formed from lower concentrations of the macromer (7.5 and 10%) were slightly opaque, whereas the hydrogel pellets formed from higher macromer concentrations were transparent (15 and 20%). This may indicate the formation of small crosslinked networks with poor solubility, leading to some

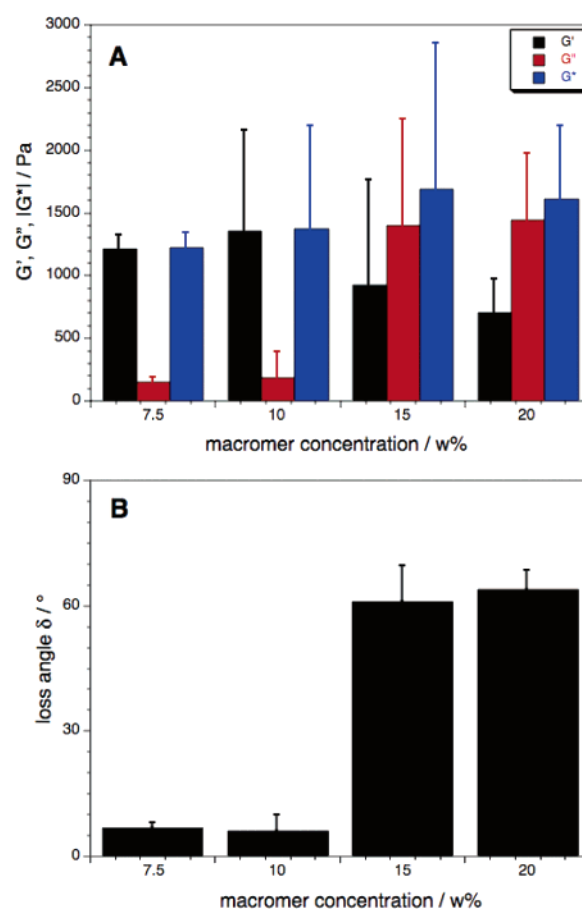


**Figure 2.** (A) Complex modulus  $|G^*|$ , storage modulus  $G'$ , and loss modulus  $G''$  for the crosslinked hydrogel samples at 4 different concentrations of macromer **1** in PBS (7.5%:  $n = 2$ , 10%:  $n = 3$ , 15%:  $n = 6$ , and 20%:  $n = 6$ ). The difference between the moduli in A is not statistically significant. (B) The loss angle  $\delta$  for crosslinked hydrogel samples at 4 different concentrations of macromer **1** in PBS (7.5%:  $n = 2$ , 10%:  $n = 3$ , 15%:  $n = 6$ , and 20%:  $n = 6$ ). Loss angles for 7.5% vs 10% and 15% vs 20% are not statistically different; however, loss angles for 15% and 20% are statistically different from loss angles for 7.5% and 10% with  $P < 0.01$ .



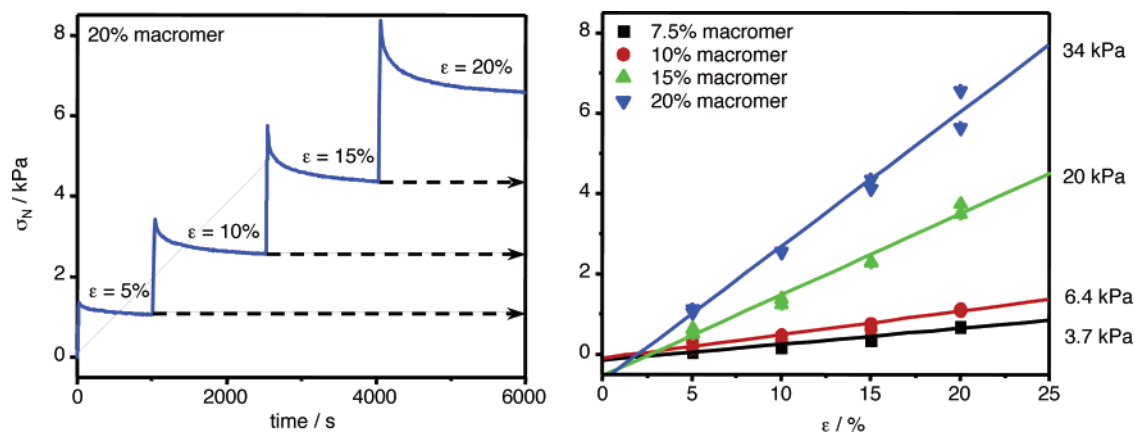


**Figure 3.** Determination of the compressive modulus  $E$ , as a function of concentration of macromer 1 in PBS. A representative compression-relaxation experiment for 20% 1 is shown on the left (A), the linear curve fits for all concentrations and the resulting compressive modulus  $E$  is shown on the right (B,  $n = 2$ ). The difference in the compressive moduli for 7.5 and 10% are not statistically significant. The other values significantly different with  $P < 0.05$  (7.5:15, 10:15, and 15:20) and  $P < 0.01$  (7.5:20 and 10:20).

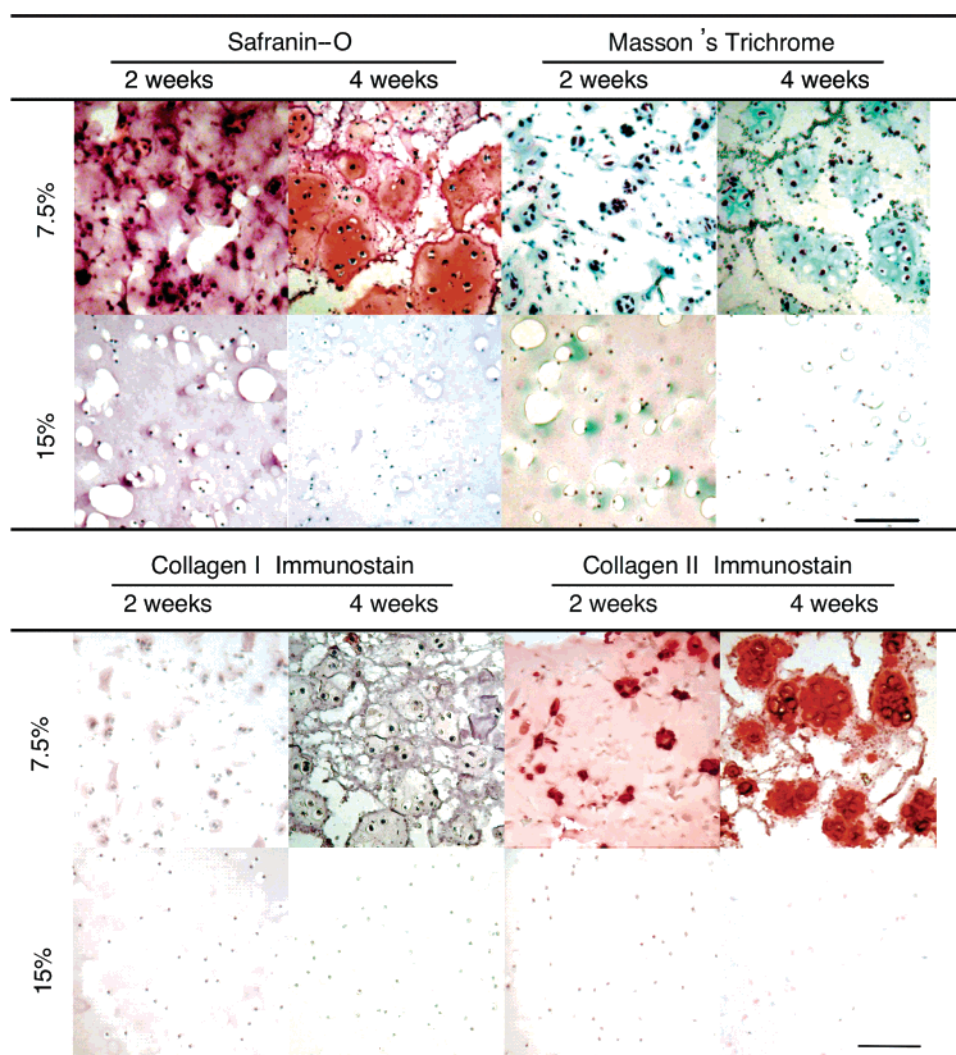


**Figure 4.** Histological sections of 7.5% and 15% macromer concentration hydrogels after 2 and 4 weeks incubation. Top: Red indicates proteoglycans in the Safranin-O stained sections, green indicates collagen in the Masson's Trichrome stained sections. Bottom: Red indicates type I or II collagen in the immunostained sections, no significant type I collagen was detected at either concentration. The length of the inserted bar is 100  $\mu\text{m}$ .

precipitation during polymerization at the lower macromer concentrations.

**Mechanical Properties.** The dynamic mechanical properties ( $G'$ ,  $G''$ ,  $|G^*|$ , and  $\delta$ ) showed no appreciable frequency dependence from 0.1 rad/s up to 100 rad/s, at all four macromer

concentrations (data not shown). The complex modulus  $|G^*|$  of the hydrogels showed only limited concentration dependence, increasing from 1.2 to 1.7 kPa, over the concentration range. The loss angle  $\delta$ , however, increased strongly from  $6.3 \pm 0.5^\circ$  at the lowest macromer concentration to  $70.6 \pm 0.3^\circ$  at the

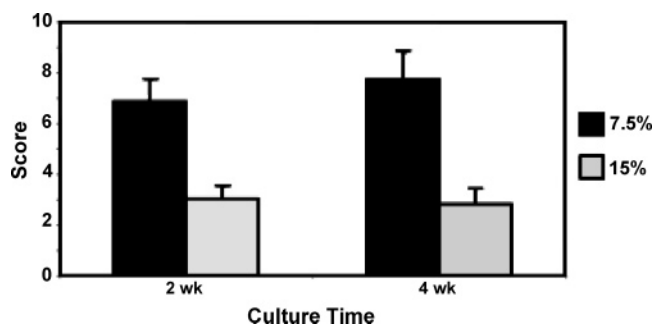


**Figure 5.** Histological grading scores for both concentrations of macromer at 2 and 4 weeks. Constructs crosslinked from the 7.5% macromer show consistently higher scores than those crosslinked from the 15% macromer.

highest macromer concentration, showing a transition from primarily elastic behavior at the lowest macromer concentration to more viscoelastic behavior at higher macromer concentrations (Figure 2).

The equilibrium compressive modulus  $E$  was determined from the equilibrium compressive stress following a stepwise increase in compressive strain (Figure 3). The compressive modulus increased significantly from  $3.7 \pm 0.1$  kPa at the lowest macromer concentration to  $34 \pm 5$  kPa at the highest macromer concentration, showing strong nonlinear stiffening of the hydrogels with increasing macromer concentration.

With values for the storage, loss, and complex modulus in the 1–2 kPa range, it is clear that the dynamic mechanical properties of the hydrogel scaffold materials are significantly lower than the values of native cartilaginous tissues in the 7–1000 kPa range. The compressive modulus in the 4–34 kPa range is comparable to values found for the nucleus pulposus (5.8 kPa) but is still significantly lower than compressive moduli for stiffer cartilaginous materials such as articular cartilage. The loss angle varies strongly with macromer concentration, but only the lower concentrations can afford the elastic properties that are required.

**Chondrocyte Encapsulation.** Histological sections prepared from cell-hydrogel constructs showed chondrocytes displaying a rounded morphology in hydrogels prepared from both the 15 and 7.5% macromer concentrations, throughout the duration of culture. After two weeks of culture, Safranin-O and Masson's Trichrome staining indicated that chondrocytes encapsulated in hydrogels at the lower macromer concentration accumulated an abundant extracellular matrix rich in proteoglycans and collagen, respectively (Figure 4). In contrast, cells encapsulated in

hydrogels at the higher macromer concentration produced extracellular matrix only in the immediate vicinity of each cell. Sections of cell-hydrogel constructs prepared from the lower macromer concentration stained strongly for type II collagen after two weeks, suggesting the accumulation of an extracellular matrix with molecular components present as found in native articular cartilage. No significant staining for type I collagen was observed (Figure 4). The cell-hydrogel constructs at lower macromer concentration also started showing histological signs of degradation, with evidence of small voids in the hydrogel scaffold. Similar voids were not apparent in the cell-hydrogel constructs formed from the higher macromer concentrations.

After four weeks of culture, the difference between the lower and higher concentration hydrogels was even more striking. The accumulation of proteoglycans and type II collagen in the lower macromer concentration samples had increased significantly and spread throughout the scaffold. The cell-hydrogel constructs formed at lower macromer concentration had lost physical integrity, with some samples disintegrating into several smaller fragments. The loss of integrity was also evident from the larger voids visible in the constructs. These cell-hydrogel constructs were fully degraded in 5–6 weeks. This behavior was not observed for the cell-hydrogel constructs formed at the higher macromer concentration, even after 12 weeks of culture (not shown). Few differences were observed between the time-points in the accumulation of extracellular matrix in the cell-hydrogel constructs at higher macromer concentration after 2, 4, or even 12 weeks (not shown) of culture.

Histological grading results show appreciably higher total scores at both 2 and 4 weeks for constructs crosslinked from the lower macromer concentration (Figure 5). Scores at 4 weeks (7.8) are about one point higher than those for 2 weeks (6.9) for the lower concentration macromer, whereas there is no difference in scores with time for the higher concentration.

**Swelling and Degradation.** No appreciable swelling was observed in any of the four concentrations during equilibration at 37 °C in PBS or chondrocyte medium after crosslinking. An initial decrease in normalized sample weight was observed, with re-swelling to 80–110% of the initial sample weight within 7 days (Figure 6). This is in sharp contrast to linear poly(ethylene glycol) dimethacrylates that can show swelling in excess of 200%. The hydrogel samples showed no significant changes in sample weight while immersed in PBS or chondrocyte medium, up to 35 days (Figure 6). In contrast to the experiments discussed previously, no loss of integrity was observed in the samples during the course of the experiment. This indicates a lack of

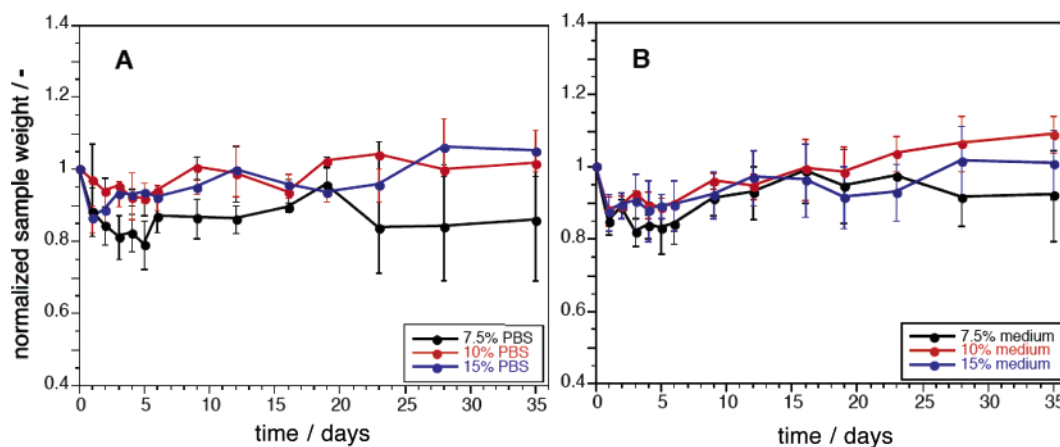


**Figure 6.** Normalized weight of hydrogel samples at 7.5, 10, and 15% macromer concentration (averaged,  $n = 3$ ), stored in PBS (A) or chondrocyte culture medium (B), at 37 °C, as a function of time.

degradation or a significant decrease in degradation rate in the absence of chondrocytes (Figure 6).

## Discussion

Hydrogels can be prepared from chemically crosslinked methacrylated macromer **1**, at a range of macromer concentrations possessing varied mechanical properties. These dendritic-based hydrogels support chondrocyte proliferation and cartilaginous tissue growth in vitro. Additionally, these hydrogels exhibit mechanical properties with higher values than previously published crosslinked alginate<sup>44</sup> and hyaluronan<sup>45</sup> hydrogels and show mechanical performance comparable to nondegradable PEG-based hydrogel systems previously reported in the literature.<sup>17,46</sup> The mechanical properties of the materials presented here approach those published recently by Bryant et al for PEG hydrogels.<sup>22–24</sup>

Excessive swelling can be detrimental to in vivo applications, because cartilage trauma sites are generally confined in geometry. When a hydrogel scaffold is formed in situ at the cartilage trauma site, the cross-linked material may swell beyond the boundaries of the trauma and may eventually detach from the wound site or exacerbate the trauma. The biodendrimer-based materials presented here demonstrated only small volume changes during crosslinking and subsequent equilibration at 37 °C in PBS or chondrocyte medium. In comparison, similar materials studied by Bryant et al., based on methacrylated PLA-block-PEG-block-PLA copolymers, show favorable mechanical properties but show volumetric swelling of 150–200%, with increased swelling during the degradation process.<sup>22–24</sup> The lack of swelling in the biodendrimer-based hydrogel materials increases our confidence in these materials as a suitable scaffold for in situ tissue engineering in confined defect sites. The low swelling ratio is likely a consequence of the multivalent nature of the macromer molecule. This feature allows multiple crosslinks per molecule, leading to a higher crosslinking density compared to a bifunctional linear molecule.

In addition to the favorable mechanical properties and low swelling, the biodendrimer-based hydrogel scaffolds support cartilaginous extracellular matrix production. Encapsulated chondrocytes show no signs of dedifferentiation; they retain their rounded morphology and produce an extracellular matrix similar to native articular cartilage, including type II collagen and proteoglycans. The lower macromer concentration hydrogel scaffolds were especially supportive of cartilaginous extracellular matrix synthesis. The more rapid synthesis of proteoglycans and collagen by chondrocytes encapsulated in the lower macromer concentration hydrogel may be due to beneficial diffusion characteristics for nutrients, waste products, oxygen, and carbon dioxide, in a hydrogel with higher water content.

The scaffold degradation rate is another important parameter for a tissue-engineering material. The degradation rate of the hydrogel–cell constructs at 7.5% macromer concentration is rapid, with rates comparable to the PLA-PEG-PLA hydrogels.<sup>22–24</sup> The hydrogel–cell constructs at the higher macromer concentration do not show appreciable degradation, even after 12 weeks in culture, impeding cell proliferation and matrix deposition. The differences in degradation kinetics are likely due to crosslink density of the hydrogels. The metabolic activity of the encapsulated chondrocytes, secreting hydrolytic enzymes is another important factor affecting degradation. The negligible degradation in the absence of cells illustrates that their presence of cells has a profound influence on degradation kinetics. This illustrates the strong impact that entrapped cells may have on

materials and underlines the importance of (degradation) experiments with relevant cells prior to in vivo experiments.

## Conclusion

The results obtained with the biodendrimer hydrogel support the strategy of using a dendritic macromolecule to control hydrogel properties and promote cartilaginous tissue formation. Even though the mechanical properties of the lower concentration hydrogels are lower than for native articular cartilage, it is clear that simply increasing the macromer concentration to improve mechanical properties is likely not the best route to a better performing scaffold. The degradation rate of the biodendrimer-based hydrogel system will need to be tuned to extracellular matrix deposition, to allow in vivo formation of neocartilaginous tissue before the matrix has fully degraded. It is clear that a compromise between targeted mechanical, diffusion and biochemical properties is necessary to afford an optimal tissue engineering scaffold for cartilage matrix production in vitro or in vivo. The photo-crosslinked scaffold presented here was designed to allow for the variation of dendrimer generation, degree of branching, crosslink density, hydrolyzable linkage, and end group functionality. This allows facile future tailoring of the physical, (bio)chemical, and mechanical properties of the scaffold for repair of cartilage defects based on specific performance requirements. The successful formation of new cartilaginous material in the biodendrimer-based hydrogel scaffold demonstrates the versatility and utility of this system, provides further incentive for the evaluation of dendritic macromolecules in other medical applications, and highlights the importance of using designer materials in tissue engineering.

**Acknowledgment.** The authors thank Netherlands Organization for Scientific Research (S.H.M.S.), NIH EB02263 (L.A.S.), OREF (M.W.G.), the Whitaker Foundation (M.W.G.), and a pre-doctoral NSF fellowship (D.L.N.) for funding.

**Supporting Information Available.** Experimental details and grading scales. This material is available free of charge via the Internet at <http://pubs.acs.org>.

## References and Notes

- (1) Moskowitz, R. W. *Osteoarthritis: diagnosis and medical/surgical management*, 2nd ed.; W. B. Saunders Company: Philadelphia, PA, 1984.
- (2) Hunziker, E. B. *Osteoarthritis. Cartilage* **2002**, *10* (6), 432–463.
- (3) Lee, C. R.; Grodzinsky, A. J.; Hsu, H. P.; Spector, M. J. *Orthop. Res.* **2003**, *21* (2), 272–281.
- (4) Klein, T. J.; Schumacher, B. L.; Schmidt, T. A.; Li, K. W.; Voegtline, M. S.; Masuda, K.; Thonar, E. J. M. A.; Sah, R. L. *Osteoarthritis. Cartilage* **2003**, *11* (8), 595–602.
- (5) van Susante, J. L. C.; Pieper, J.; Buma, P.; van Kuppevelt, T. H.; van Beuningen, H.; van der Kraan, P. M.; Veerkamp, J. H.; van den Berg, W. B.; Veth, R. P. H. *Biomaterials* **2001**, *22* (17), 2359–2369.
- (6) Chenite, A.; Chaput, C.; Wang, D.; Combes, C.; Buschmann, M. D.; Hoemann, C. D.; Leroux, J. C.; Atkinson, B. L.; Binette, F.; Selmani, A. *Biomaterials* **2000**, *21* (21), 2155–2161.
- (7) Silverman, R. P.; Bonasser, L.; Passaretti, D.; Randolph, M. A.; Yaremchuk, M. J. *Plast. Reconstruct. Surg.* **2000**, *105* (4), 1393–1398.
- (8) Brun, P.; Cortivo, R.; Zavan, B.; Vecchiato, N.; Abatangelo, G. J. *Mater. Sci.-Mater. Med.* **1999**, *10* (10–11), 683–688.
- (9) Brun, P.; Abatangelo, G.; Radice, M.; Zacchi, V.; Guidolin, D.; Daga Gordini, D.; Cortivo, R. J. *Biomed. Mater. Res.* **1999**, *46* (3), 337–46.
- (10) Silverman, R. P.; Passaretti, D.; Huang, W.; Randolph, M. A.; Yaremchuk, M. J. *Plast. Reconstruct. Surg.* **1999**, *103* (7), 1809–1818.



- (11) Paige, K. T.; Cima, L. G.; Yaremchuk, M. J.; Vacanti, J. P.; Vacanti, C. A. *Plast. Reconstruct. Surg.* **1995**, 96 (6), 1390–1398.
- (12) Cao, T.; Ho, K. H.; Teoh, S. H. *Tissue Eng.* **2003**, 9, S103–S112.
- (13) Moran, J. M.; Pazzano, D.; Bonassar, L. J. *Tissue Eng.* **2003**, 9 (1), 63–70.
- (14) Schaefer, D.; Martin, I.; Jundt, G.; Seidel, J.; Heberer, M.; Grodzinsky, A.; Bergin, I.; Vunjak-Novakovic, G. *Arthritis Rheumatism* **2002**, 46 (9), 2524–2534.
- (15) Freed, L. E.; Grande, D. A.; Lingbin, Z.; Emmanuel, J.; Marquis, J. C.; Langer, R. J. *Biomed. Mater. Res.* **1994**, 28 (8), 891–899.
- (16) Temenoff, J. S.; Park, H.; Jabbari, E.; Conway, D. E.; Sheffield, T. L.; Ambrose, C. G.; Mikos, A. G. *Biomacromolecules* **2004**, 5 (1), 5–10.
- (17) Elisseeff, J.; McIntosh, W.; Anseth, K.; Riley, S.; Ragan, P.; Langer, R. J. *Biomed. Mater. Res.* **2000**, 51 (2), 164–171.
- (18) Elisseeff, J.; Anseth, K.; Sims, D.; McIntosh, W.; Randolph, M.; Langer, R. *Proc. Natl. Acad. Sci. U.S.A.* **1999**, 96 (6), 3104–3107.
- (19) Elisseeff, J.; Anseth, K.; Sims, D.; McIntosh, W.; Randolph, M.; Yaremchuk, M.; Langer, R. *Plast. Reconstruct. Surg.* **1999**, 104 (4), 1014–1022.
- (20) Guilak, F.; Kapur, R.; Sefton, M. V.; Vandenburgh, H. H.; Koretsky, A. P.; Kriete, A.; O'Keefe, R. J. *Ann. N. Y. Acad. Sci.* **2002**, 961, 207–209.
- (21) Halstenberg, S.; Panitch, A.; Rizzi, S.; Hall, H.; Hubbell, J. A. *Biomacromolecules* **2002**, 3 (4), 710–723.
- (22) Bryant, S. J.; Anseth, K. S. *J. Biomed. Mater. Res.* **2003**, 64A (1), 70–79.
- (23) Martens, P. J.; Bryant, S. J.; Anseth, K. S. *Biomacromolecules* **2003**, 4 (2), 283–292.
- (24) Bryant, S. J.; Durand, K. L.; Anseth, K. S. *J. Biomed. Mater. Res.* **2003**, 67A (4), 1430–1436.
- (25) Wilson, C. G.; Bonassar, L. J.; Kohles, S. S. *Arch. Biochem. Biophys.* **2002**, 408 (2), 246–254.
- (26) Fréchet, J. M. J. *Proc. Natl. Acad. Sci. U.S.A.* **2002**, 99 (8), 4782–4787.
- (27) Fréchet, J. M. J.; Tomalia, D. A. *Dendrimers and other dendritic polymers*; John Wiley & Sons: New York, 2002; p 648.
- (28) Grayson, S. M.; Fréchet, J. M. J. *Chem. Rev.* **2001**, 101 (12), 3819–3867.
- (29) Newkome, G. R.; Moorefield, C. N.; Vögtle, F. *Dendrimers and dendrons: concepts, synthesis, perspectives*; Wiley-VCH: Weinheim, Germany, 2001.
- (30) Bosman, A. W.; Janssen, H. M.; Meijer, E. W. *Chem. Rev.* **1999**, 99 (7), 1665–1688.
- (31) Fisher, M.; Vögtle, F. *Angew. Chem., Int. Ed.* **1999**, 38 (7), 884–905.
- (32) Majoral, J. P.; Caminade, A. M. *Chem. Rev.* **1999**, 99 (3), 845–880.
- (33) Matthews, O. A.; Shipway, A. N.; Stoddart, J. F. *Prog. Polym. Sci.* **1998**, 23 (1), 1–56.
- (34) Zheng, F.; Zimmerman, S. C. *Chem. Rev.* **1997**, 97 (5), 1681–1712.
- (35) Newkome, G. R.; Moorefield, C. N.; Keith, J. M.; Baker, G. R.; Escamilla, G. H. *Angew. Chem., Int. Ed.* **1994**, 33 (6), 666–668.
- (36) Issberner, J.; Moors, R.; Vögtle, F. *Angew. Chem., Int. Ed.* **1994**, 33, 2413–2420.
- (37) Vögtle, F. *Dendrimers*. Springer: Berlin, 1998; Vol. 197, p 240.
- (38) Vögtle, F. *Dendrimers II: Architecture, Nanostructure and Supramolecular Chemistry*; Springer: Berlin, 2000; Vol. 210, p 311.
- (39) Vögtle, F. *Dendrimers III: Design, Dimension, Function*; Springer: Berlin, 2001; Vol. 212, p 198.
- (40) Grinstaff, M. W. *Chem. Eur. J.* **2002**, 8 (13), 2839–2846.
- (41) Carnahan, M. A.; Grinstaff, M. W. *J. Am. Chem. Soc.* **2001**, 123 (12), 2905–2906.
- (42) Carnahan, M. A.; Middleton, C.; Kim, J.; Kim, T.; Grinstaff, M. W. *J. Am. Chem. Soc.* **2002**, 124, 5291–5293.
- (43) Kuettner, K.; Pauli, B.; Gall, G.; Memoli, V.; Schenk, R. *J. Cell. Biol.* **1982**, 93 (3), 743–50.
- (44) LeRoux, M. A.; Guilak, F.; Setton, L. A. *J. Biomed. Mater. Res.* **1999**, 47 (1), 46–53.
- (45) Smeds, K. A.; Grinstaff, M. W. *J. Biomed. Mater. Res.* **2001**, 54 (1), 115–121.
- (46) Bryant, S. J.; Anseth, K. S. *J. Biomed. Mater. Res.* **2002**, 59 (1), 63–72.
- (47) Setton, L. A.; Elliot, D. M.; Mow, V. C. *Osteoarthr. Cartilage* **1999**, 7, 2–14.
- (48) Setton, L. A.; Mow, V. C.; Howell, D. S. *J. Orthop. Res.* **1995**, 12 (4), 437–82.
- (49) Iatridis, J. C.; Weidenbaum, M.; Setton, L. A.; Mow, V. C. *Spine* **1996**, 21 (10), 1174–1184.
- (50) Umehara, S.; Tadano, S.; Abumi, K.; Katagiri, K.; Ukai, T. *Spine* **1996**, 21 (7), 811–819.

BM050663E